Article

Substrate-Assisted Hydroxylation and O-Demethylation in the Peroxidase-Like Cytochrome P450 Enzyme CYP121

Romie C. Nguyen, Yu Yang, Yifan Wang, Ian Davis, and Aimin Liu

ACS Catal., **Just Accepted Manuscript** • DOI: 10.1021/acscatal.9b04596 • Publication Date (Web): 20 Dec 2019

Substrate-Assisted Hydroxylation and *O*-Demethylation in the Peroxidase-Like Cytochrome P450 Enzyme CYP121

Romie C. Nguyen, Yu Yang, Yifan Wang, Ian Davis, and Aimin Liu*

Department of Chemistry, University of Texas, San Antonio, Texas 78249, United States

***Editorial correspondence to**:

Aimin Liu

Department of Chemistry

The University of Texas at San Antonio

1 UTSA Circle

San Antonio, TX 78249-0698

Phone: +1-210-458-7062; Fax: 210-458-7428

*E-mail: Feradical@utsa.edu

ABSTRACT

CYP121 is a P450 enzyme from *Mycobacterium tuberculosis* that catalyzes a C-C coupling reaction between the two aromatic rings on its native substrate cyclo(L-Tyr-L-Tyr) (cYY) to form mycocyclosin, a necessary product for cell survival. Unlike the typical P450 enzymes for hydroxylation, CYP121 is believed to behave like a peroxidase and conduct radical-mediated C-C bond formation. Here, we probe whether the phenolic hydrogen of the substrate is the site of the postulated hydrogen atom abstraction for radical formation. We synthesized a singly *O*-methylated substrate analog, cYF-4-OMe, and characterized its interaction with CYP121 by UV-vis, EPR, and X-ray crystallography. We found that cYF-4-OMe can function as a substrate of CYP121 using the established assay *via* the peroxide shunt. Analysis of the enzymatic reaction revealed an *O*-demethylation of cYF-4-OMe instead of cyclization, yielding cYY and formaldehyde. A hydroxylated substrate, cYF-4-OMeOH, is expected to be the intermediate product, which was trapped and structurally characterized by X-ray crystallography. We further determined that the deformylation reaction of cYF-4-OMeOH proceeds *via* an alkyl–O, rather than aryl−oxygen, bond cleavage by the ^{18}O-labeling studies. Finally, the pH-dependence catalytic study on the native substrate and the methoxy analog further support the mechanistic understanding that the hydrogen atom abstraction is the critical first oxidation step exerted by a heme-based oxidant during the cyclization reaction of cYY. The switch in catalytic activity reveals the power of CYP121 as a P450 enzyme and provides insight into the peroxidase-like catalytic mechanism.

KEY WORDS: catalytic mechanism, heme, oxygen activation, P450, and tuberculosis

INTRODUCTION

The cytochrome P450 enzyme, CYP121, from *Mycobacterium tuberculosis* (Mtb) is essential for viability of the pathogen[1], *i.e.*, the causative agent of tuberculosis. Knock out of the corresponding gene of CYP121 leads to the inability of Mtb to grow. Hence, CYP121 has been recognized as a potential drug target against tuberculosis.[2] P450 enzymes are commonly categorized as monooxygenases, performing an oxygen insertion reaction to a variety of substrates.[3] However, CYP121 catalyzes an unusual intramolecular C-C bond crosslinking reaction that cyclizes the substrate cyclo(L-Tyr-L-Tyr) (cYY) to give rise to the product mycocyclosin (Scheme 1A).[4] The C-C coupling reaction has been observed in plant and bacterial P450 enzymes[5], some of which include CYP245A1 StaP from *Streptomyces* sp. TP-A0274 which forms the indolecarbazole core of the anti-tumor agent staurosporine[6], CYP719B1 and CYP80G2 where both enzymes mediate intramolecular phenol coupling to form plant secondary metabolites[7-8], and OxyC, the P450 involved in aryl ring coupling in the biosynthesis of the antibiotic vancomycin.[9] However, mechanistic understanding is lacking for the catalytic activity for any of the above P450 enzymes.

A diradical-based C-C bond formation reaction is anticipated for the CYP121-mediated reaction.[4, 10-11] A quantum mechanics/molecular mechanics computational study also invokes the diradical mechanism.[11] Although the substrate-based radical intermediate remains to be trapped and characterized, its participation in the catalytic cycle is analogous to similar C-C bond formation from two aromatic residues in the biogenesis of the tryptophan tryptophylquinone cofactor in methylamine dehydrogenase.[12] The diradical mechanism is also supported by experimental evidence on alternate substrates. CYP121 is found to possess peroxidase-like

catalytic activity capable of oxidizing peroxidase substrates to their radical forms,and is therefore labeled a P450 peroxidase.[10]

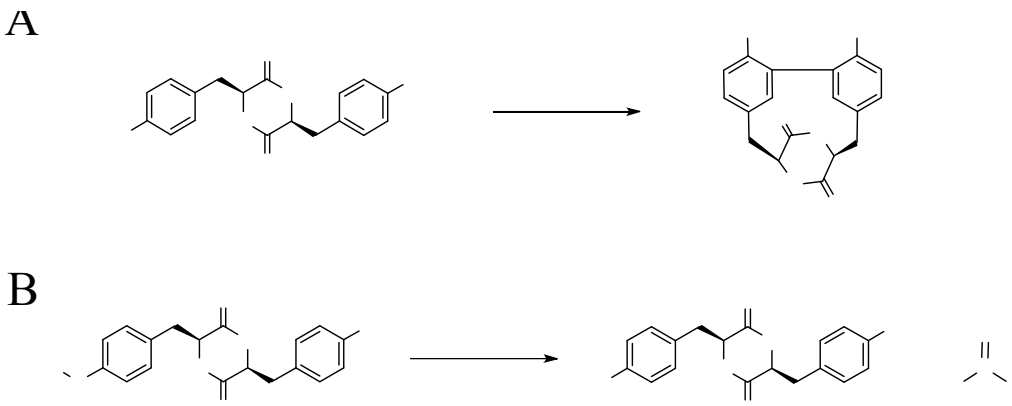

Scheme 1. Reaction of CYP121 with native substrate (A) cYY to form mycocyclosin via a C-C bond coupling cyclization reaction and (B) designed synthetic probe cYF-4-OMe to form cYY as a product.

The catalytic center of CYP121 is a heme-thiolate which is similar to other P450 enzymes. The co-crystallized CYP121-cYY complex shows that cYY binds with its phenol groups at nearly 90° to each other. This binding of cYY minimally alters the structure of the enzyme and causes nearly non-observable changes in the active site architecture.[1, 4] In the first step of a general P450 mechanism, substrate binding results in loss of the axial water ligand leading to an open coordination site to the heme iron, converting it from a six-coordinate low-spin ferric state to a five-coordinate high-spin species for further reduction and O_2 binding.[13-14] However, this is not the case for CYP121. The CYP121-cYY complex remains mostly at the low-spin ferric state and the high-spin species is minimal as measured by EPR and UV-vis spectroscopies.[15] To understand these observations that are contrary to how P450 enzymes generally behave upon substrate binding, an ENDOR spectroscopic study of CYP121 has been described in our previous study. The solvent-derived distal ligand at the ferric heme iron ion is shown to be in dynamic equilibrium among water, hydroxide, and the ligand-free form, which is

affected by temperature and pH.[15] The binding of cYY to the distal pocket of the heme alters the equilibrium and weakens the solvent-derived ligand affinity to the iron ion but does not cause a purely ligand-free heme center, yet the heme has a 100-fold higher affinity to cyanide than the enzyme alone without cYY.[15]

The lack of active site reorganization upon cYY binding does not follow the general P450 mechanism, possibly due to CYP121 not being a metabolic enzyme and requiring less efficient catalytic activity. Nonetheless, the catalytic pathway of CYP121 has been shown to largely resemble the well-established P450 mechanism at the early steps of the cycle through demonstration that the peroxide shunt pathway is operative.[10] This pathway commonly utilizes hydrogen peroxide to generate product, though other peroxides such as peracetic acid are also known to be effective.[10] Use of a peroxide implicates formation of firstly a hydroperoxo, then a high-valent ferryl species coupled with a heme or protein radical (i.e., Compound I) during catalysis.[10] For all proposed mechanisms thus far, the hydrogen atom from the hydroxyl group of the tyrosine moiety adjacent to the heme is proposed to be abstracted by a ferryl-oxo species, forming a radical on the substrate, cYY$^{\bullet}$ as the first step of the oxidation.[4, 10-11] However, there is no experimental evidence thus far for the postulated hydrogen abstraction event during catalysis. The absence of experimental evidence to differentiate between a concerted or stepwise diradical formation constitutes a knowledge gap in the understanding of the cyclization mechanism of cYY by CYP121.

In the present work, we aim to probe the first catalytic step of the CYP121 pathway after the formation of the enzyme-based oxidant. A single tyrosine moiety of the substrate was modified from a phenol to an aryl methoxy group to probe the ability of the enzyme to handle the lack of an easily removable hydrogen atom. The investigation of the synthetic probe with

CYP121-mediated reaction not only confirmed the catalytic importance of the hydroxyl group of cYY during the initial step of catalytic oxidation mediated by a heme-based oxidant, but also yielded a surprising outcome that elucidates the intrinsic P450 catalytic characteristics of the heme center in this peroxidase-like P450 enzyme.

RESULTS

The enzyme-substrate interaction with the synthetic probe cyclo(L-Tyr-L-Phe-4-OMe)

Cyclo(L-Tyr-L-Phe-4-OMe) (cYF-4-OMe) is a cyclodipeptide in the L-configuration with a single tyrosine moiety modified to phenylalanine with a methoxy group located in the fourth position on the phenyl ring. This modification was chosen to interrogate the importance and role of the hydroxyl group in the catalytic cycle of CYP121. The compound was synthesized using previously published methods on chiral piperazine synthesis with minor modifications (*Supporting Information*, Scheme S1).[10, 16-17] The characterization of this synthetic probe by mass spectrometry and NMR spectroscopy is described in Figure S1.

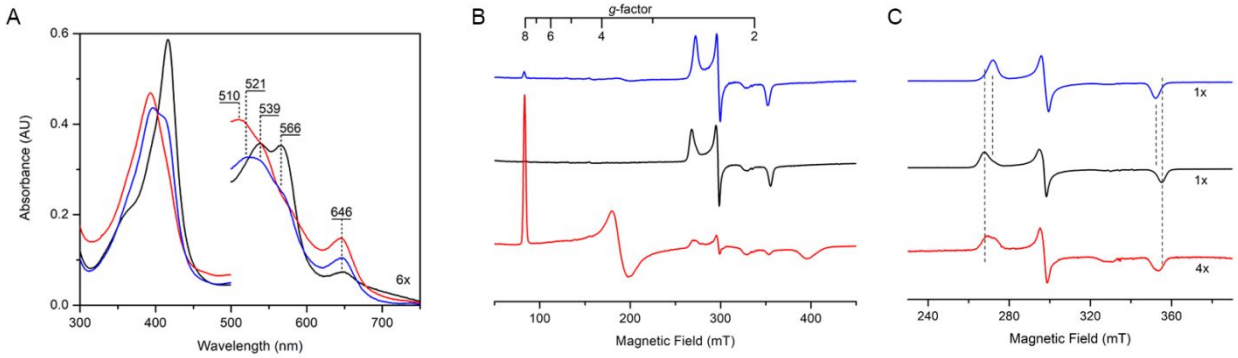

Figure 1. Binding characteristics of cYY and cYF-4-OMe with CYP121 as measured by UV-vis and EPR spectroscopies. CYP121 bound with no added ligand (black), cYY (blue), and cYF-4-OMe (red) was measured by: **A**, UV-vis spectroscopy of ferric form of CYP121 (5 μM) with cYY (300 μM) or cYF-4-OMe (100 μM); **B**, EPR spectroscopy of CYP121 (200 μM) at 10 K, 1 mW with cYY (400 μM) or cYF-4-OMe (200 μM); and **C**, The $g = 2$ region EPR spectra at 50 K, 0.2 mW. A spectral shift is observed upon ligand binding. Note that full binding is not achieved for cYF-4-OMe due to the low solubility in buffer which presents itself as a shoulder that is similar to unbound enzyme.

The binding of cYF-4-OMe to CYP121 shares similar spectroscopic characteristics with cYY in the electronic absorption spectrum (Figure 1A). In the absence of a ligand, CYP121 exhibits an expected Soret band centered at 416 nm with a shoulder at 358 nm as well as α/β bands at 539 nm and 566 nm.[4, 10] Upon addition of cYF-4-OMe, the Soret band blue shifts from 416 nm to 394 nm, a more pronounced version of the shift caused by cYY binding which is indicative of Type I binding where a water ligand is displaced from the heme iron. Differences are also observed in the α/β region for both cYY and cYF-4-OMe binding, where the 538 nm and 565 nm peaks become broadened. The broad feature in the cYF-4-OMe-enzyme complex is similar in shape to the feature seen in cYY binding, yet it is slightly blue shifted with an observable increase in signal intensity. The charge transfer band at 645 nm is observed in the spectrum of both compounds, though the cYF-4-OMe band has higher absorbance than with cYY. Overall, cYF-4-OMe binding causes more observable changes of the electronic structure of the heme center compared to changes caused by cYY binding.

EPR spectroscopic characterization revealed a more pronounced spectral change upon cYF-4-OMe binding as compared to cYY. In the EPR spectrum of cYF-4-OMe bound to CYP121, a large high-spin ferric signal (g_x 1.69, g_y 3.55, and g_z 8.04) that is absent from free enzyme and minor in the CYP121-cYY complex, is observed coupled with a decrease in the low-spin signal of the ferric heme in the resting state (Figure 1B). The low- to high-spin conversion, which is missing from the binding of the native substrate cYY,[10, 15] indicates either the loss of a solvent-derived axial ligand from the ferric heme or substantially weakened binding to the heme upon binding of the synthetic probe. However, such a new high-spin ferric heme EPR signal of CYP121 is commonly seen in many other P450 enzyme-substrate complexes with typical hydroxylation catalytic activities.[18-19]

The minor rhombic, low-spin ferric heme species of the enzyme-probe complex were measured at non-saturating conditions for the low-spin species (50 K and 0.20 mW) to ensure accurate line shapes and intensities for comparison (Figure 1C). The low-spin ferric heme signal in the cYY-bound enzyme (g_x 1.90, g_y 2.25, g_z 2.46) and ligand-free (g_x 1.88, g_y 2.25, g_z 2.50) present distinct *g* values. The enzyme-substrate complex of low-spin EPR signal also has a slightly decreased rhombicity, *i.e.* Δg ($g_z - g_x$). These results suggest that the synthetic probe cYF-4-OMe binds to the heme distal pocket and causes the departure of the solvent-derived ligand as the major conformation and a minor fraction retains the solvent-derived ligand. The EPR spectra showed a near but not full conversion to the bound state upon addition of cYF-4-OMe (Figure 1C). The minor low-spin EPR signal consists of two sets of EPR signals with an approximate 2:1 ratio, one of which is identical to that of the resting enzyme. The appearance of this heterogeneity is likely due to the low solubility of cYF-4-OMe in buffer as compared to cYY, resulting in incomplete binding to the active site. This minor low-spin signal was compared to the low-spin signals of free enzyme and CYP121-cYY complex to observe differences in the bound and unbound structures. Estimate of the low-spin signal intensities yielded the relative percentages of low-spin heme in the samples as 100% for CYP121 alone, 97% for the CYP121-cYY complex, and 15% for the CYP121-cYF-4-OMe complex meaning 85% of which is in the high-spin state. It should be noted that the EPR detection of a major high-spin ferric heme ES complex and a minor low-spin species is in accord with our previous conclusion for the presence of a dynamic equilibrium state of water, -OH, and unbound heme.[15]

Table 1. Data collection and refinement statistics for cYF-4-OMe crystal structure and its hydroxylated intermediate cYF-4-OMeOH

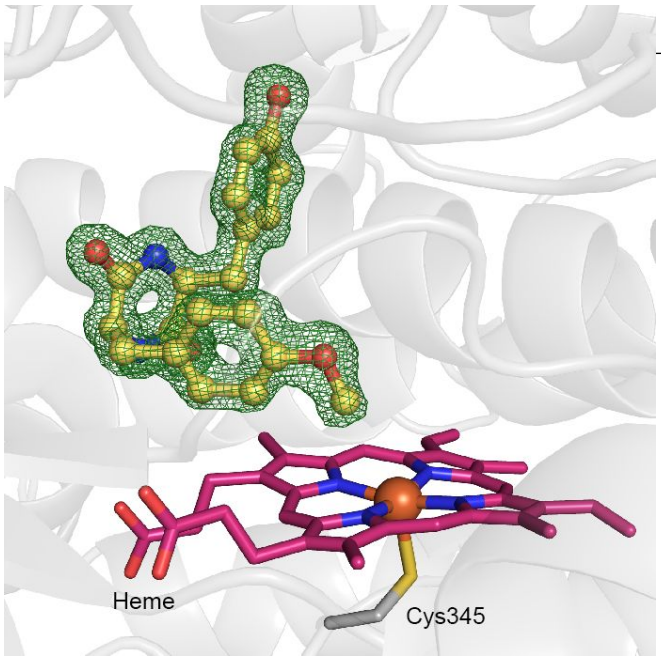

Figure 2. Co-crystallized structure of CYP121 in complex with cYF-4-OMe at 1.39 Å resolution. The $F_o - F_c$ density map (green)was contoured to 3 σ and the density was fitted with the ligand structure (yellow). A single binding orientation of the synthetic probe was observed in the active site with the methoxy group pointing to the heme.

cYF-4-OMeOH

A crystal structure of CYP121 in complex with cYF-4-OMe (Figure 2) was obtained through co-crystallization and refined to 1.39 Å resolution (Table 1). At pH 7.4, the crystal structure shows that cYF-4-OMe binds exclusively with the methyl group pointing towards the heme. This is consistent with all but one, *i.e.* cyclo(L-Tyr-L-DOPA), of the known substrate analogs thus far reflecting the scaffold of cYY bound in the distal pocket of CYP121,[20] suggesting a specific protein-cYY interaction at the remote tyrosine moiety and a relatively relaxed environment near the heme center for the primary substrate and external oxidant. Interestingly, the presence of the methyl group on cYF-4-OMe pointing towards the heme does not show any electron density above the heme iron, where a water ligand was seen in the substrate-free structure. The lack of this additional small electron density is contrary to the EPR data presented above and is likely due to low occupancy. The EPR data suggests that a very minor fraction of the probe-bound CYP121 remains to be associated with a solvent-derived

data collection		
space group	$P6_522$	$P6_522$
cell dimensions		
a, b, c (Å)	77.5, 77.5, 262.6	77.4, 77.4, 262.0
α, β, γ (deg)	90, 90, 120	90, 90, 120
resolution (Å)	50.00–1.39 (1.41–1.39)[a]	50.00–1.81 (1.84–1.81)
total reflections	93972 (3961)	42872 (2792)
unique reflections	4652 (205)	6213 (388)
redundancy	20.2 (19.3)	6.9 (7.2)
completeness (%)	99.2 (85.5)	98.3 (97.7)
$I/\sigma(I)$	28.8 (6.2)	19.3 (1.5)
R_{merge} (%)[b]	12.8 (38.9)	11.9 (96.9)
R_{pim}	0.029 (0.087)	0.049 (0.357)
$CC_{1/2}$[c]	0.996 (0.95)	0.996 (0.782)
refinement[d]		
R_{work}	17.8	18.5
R_{free}	18.8	22.5
RMSD bond length (Å)[e]	0.005	0.006
RMSD bond angles (Å)	0.899	0.959
Ramachandran statistics[f]		
preferred (%)	99.5	99.2
allowed (%)	0.5	0.8
outliers (%)	0	0
average *B*-factor (Å^2)	18.6/3688	24.5/3455
protein/atoms	17/3015	23.9/3011
heme/atoms	13.3/43	19.3/43
ligand/atoms	15.4/25	23.8/26
solvent/atoms	26.0/545	30.3/335
PDB entry	6UPG	6UPI

[a] Values in parentheses are for the highest resolution shell

[b] $R_{merge} = \sum_{hkl}\sum_i |I_i(hkl) - I(hkl)| / \sum_{hkl}\sum_i I_i(hkl)$, in which the sum is over all the *i* measured reflections with equivalent Miller indices *hkl*, *I*(*hkl*) is the averaged intensity of these *i* reflections, and the grand sum is over all measured reflections in the data set

[c] According to Karplus and Diederichs[21]

[d] All positive reflections were used in the refinement

[e] According to Engh and Huber[22]

[f] Calculated by using MolProbity[23]

ligand at the distal side of the heme, rendering it unobservable in X-ray crystallography. Together with the previous EPR/ENDOR study,[15] the solvent-derived ligand should weaken in its interaction with the heme iron in this minor fraction of the complex. The high-resolution crystal structure of the enzyme-probe complex is thus in agreement with the EPR characterization of the heme center.

Synthetic probe as an alternate substrate

The catalytic activity of CYP121 with cYF-4-OMe was probed using the previously established peroxide shunt pathway using H_2O_2 or peracetic acid as the oxidant.[10] This reaction resulted in the appearance of a single detectable new peak in the HPLC chromatogram, which eluted with a retention time of 6.3 min compared to the retention time of cYF-4-OMe at 8.3 min (Figure 3A). This new eluate has the same retention time with cYY on the column under the same conditions, and it has an $[MH]^+$ ion *m/z* 327, the same mass that has been reported previously for cYY (Figure S1B). The new eluate at 6.3 min was also analyzed by UV-vis, and the absorbance spectrum matches the known optical spectrum of cYY (Figure 3B). These results point towards loss of a methyl group from cYF-4-OMe and formation of cYY as the product of the CYP121-mediated reaction, suggesting an oxidative C-O bond cleavage event that is rarely observed for a P450 enzyme.

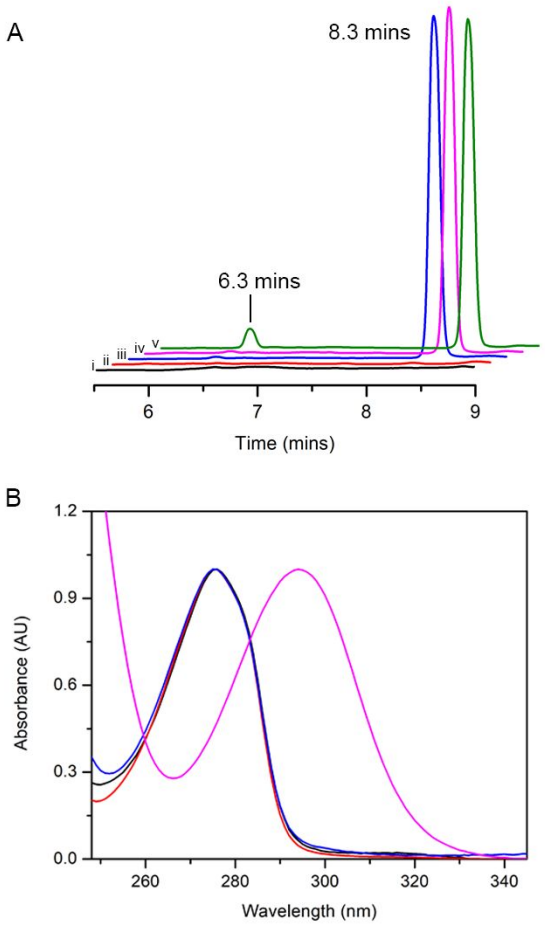

Figure 3. Reaction separation and product analysis of CYP121 and cYF-4-OMe reaction. **A**, HPLC chromatogram with detection of a peak at 6.3 min. CYP121 (**E**) and cYF-4-OMe were mixed in the presence of peracetic acid which yielded a new eluate at 6.3 min. Four controls were included: i) **E** only, ii) **E** and peracetic acid, iii) **E** and cYF-4-OMe, iv) cYF-4-OMe and peracetic acid, and v) reaction mixture of **E**, cYF-4-OMe, and peracetic acid. **B**, Normalized absorbance spectrum of cYY (blue), mycocyclosin (magenta), cYF-4-OMe (red), and the elution product at 6.3 min (black).

Identification of the secondary product of the CYP121 reaction with cYF-4-OMe

Depending on the mechanism for cYY formation from cYF-4-OMe, methanol or formaldehyde may be formed. If CYP121 follows a peroxidase-like reaction with the alternate substrate, methanol would be formed. Conversely, formaldehyde can be formed if the enzyme follows a classic P450-type reaction. Depending on the site of C-O bond cleavage, either product may be

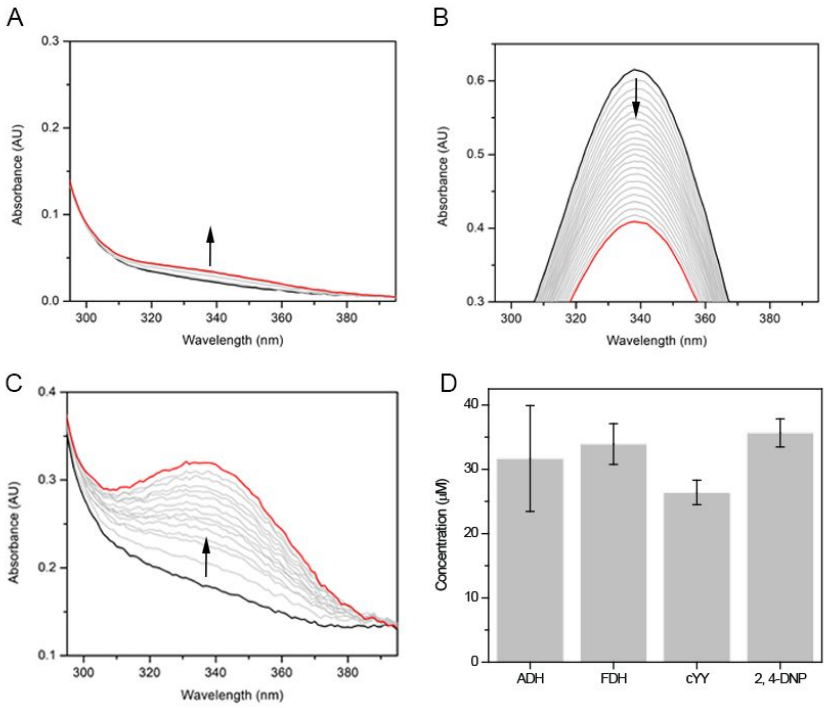

Figure 4. Methanol or formaldehyde detection and quantification from the reaction of CYP121 and cYF-4-OMe using ADH and FDH. **A**, ADH and NAD^+ to detect methanol. **B**, ADH and NADH to detect formaldehyde. **C**, FDH with NAD^+ to detect formaldehyde. **D**, Quantitation of formaldehyde using ADH, FDH, and 2, 4-DNP,compared to cYY formed.

possible. To differentiate between these two scenarios, coupled enzyme assays were performed using alcohol dehydrogenase (ADH) and formaldehyde dehydrogenase (FDH), which can be used to detect the presence of methanol or formaldehyde depending on whether NAD^+ or NADH is used as the cofactor.[24-25] The ADH reaction is bidirectional depending the availability of the cofactor, whereas the FDH reaction is unidirectional. After the CYP121 reaction was completed

with cYF-4-OMe and peracetic acid, CYP121 was removed with a 10 kDa cutoff membrane filter in a concentrator and ADH or FDH (10 μM) and NAD^+ or NADH (200 μM) was mixed with the flow through, and the absorbance was monitored at 339 nm for NADH formation or loss, respectively.

All attempts to detect and quantify methanol as a side reaction product were unsuccessful. No notable formation of NADH was observed from the reaction mixture containing ADH and NAD^+ (Figure 4A). However, when testing for the presence of formaldehyde by running the ADH reaction in reverse, a decrease in NADH absorbance was observed (Figure 4B). As illustrated in Scheme 1B, these assay results support the formation of formaldehyde as the secondary product of the CYP121-mediated cYF-4-OMe oxidation reaction. The values of the initial and final absorbance were converted to concentration of NADH using a NADH standard curve (Figure S2A) and then subtracted to yield the concentration of formaldehyde. The FDH control showed 21.4 ± 3.6 μM loss of NADH via light induced oxidation (Figure S3) and the experimental assay yielded a total loss of 59.8 ± 14.4 μM NADH. Subtracting these values gives a final calculated concentration of 31.6 ± 8.2 μM loss of NADH (Figure 4B). A cYY calibration curve (Figure S2B) was then used to calculate the concentration of product yielded from the CYP121 reaction, which gave rise to 26.4 ± 1.9 μM (Figure 4D).

To confirm the presence of formaldehyde with a more specific assay, FDH was combined with NAD^+ and added to the CYP121 reaction flow through as described above. As seen in Figure 4C, the production of NADH (33.9 ± 3.2 μM) was observed when monitoring the absorbance at 339 nm when compared to the control reaction without formaldehyde.

Because of its ubiquitous presence, formaldehyde is notoriously difficult to analyze. Therefore, we employed a third method to quantifying formaldehyde formation.[26] A third

confirmation method was employed using the known aldehyde and ketone coupling agent 2 ,4-dinitrophenylhydrazine (2, 4-DNP).[27] The formaldehyde-coupled product was observed as a new peak in HPLC (Figure S4) and a calibration curve was used to quantify the formaldehyde-coupled product (Figure S5) which yielded $35.7 \pm 2.2\ \mu$M. Together, we conclude an *O*-demethylation reaction instead of C-C bond coupling occurs when cYF-4-OMe is used in place of cYY as the substrate for CYP121.

An intermediate crystal structure captured during *in crystallo* chemical reaction

In order to provide evidence that a hydroxylation takes place at the methyl group of the probe followed by an *O*-demethylation reaction, the co-crystallized CYP121-cYF-4-OMe crystals were soaked in a mother liquor at pH 7.4 with 20% glycerol. H_2O_2 was added and crystals were soaked for 30 s to 10 min before being flash cooled in liquid nitrogen. Among the X-ray diffraction datasets collected, a potential reaction intermediate was obtained *in crystallo* as described below, and it was not otherwise populated.

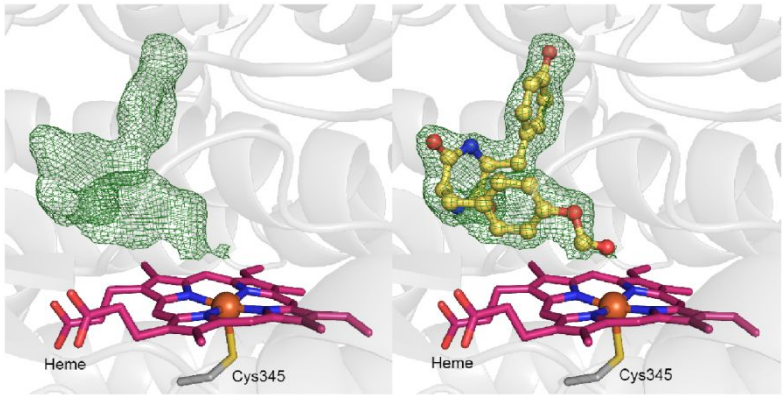

Figure 5. The crystal structure of a hydroxylated intermediate in the active site of CYP121 at 1.81 Å resolution after soaking in H_2O_2 for two minutes. The $F_o - F_c$ density map (green) is contoured to 2.5 σ (left) and the intermediate structure is modeled into the $F_o - F_c$ density map (right).

A putative intermediate was captured after soaking CYP121 co-crystallized with cYF-4-OMe with H_2O_2 for two min (Figure 5) and refined to 1.81 Å resolution (Table 1). Initially, small excess density was noticed tailing off the methoxy group towards the heme that was not observed in the CYP121-cYF-4-OMe complex. Refinement with cYF-4-OMe did not present a full account for the unoccupied electron density connected to the methoxy group. Fitting the ligand lead to a 50:50 occupancy of cYF-4-OMe and cYF-4-OMeOH, which eliminated the

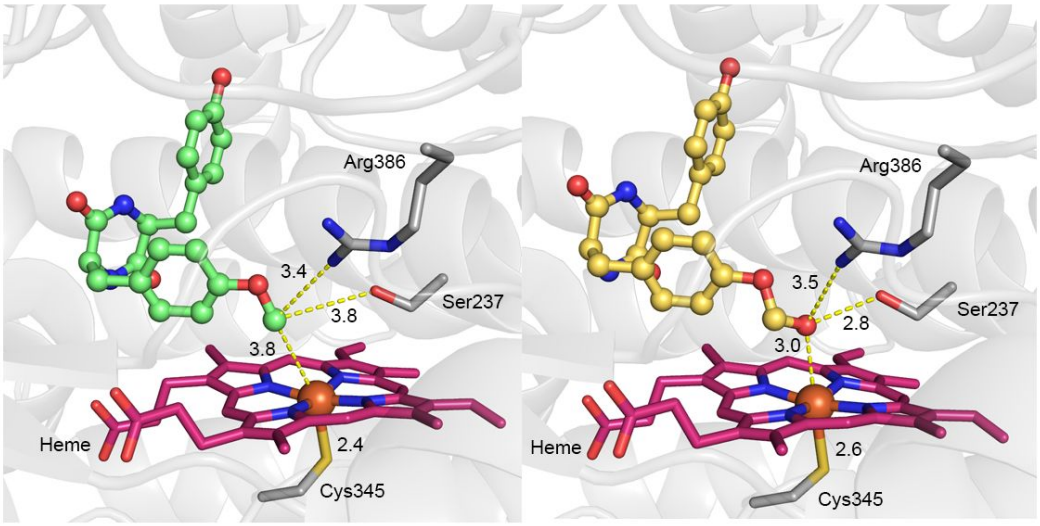

Figure 6. Structural comparison between co-crystallized structure (left, green) and the putative hydroxylated intermediate (right, yellow).

excess density. The bond distances from the intermediate structure to Ser237, Arg386, and to the heme for both the probe and its intermediate structure are shown in Figure 6. The bond length from the iron ion to the cysteine ligated residue changed from 2.4 Å in the co-crystallized structure to 2.6 Å in the proposed intermediate. Heme ruffle was measured for both the co-crystallized complex and the putative intermediate as seen in Figure S6. The co-crystallized complex yielded angles of 163.2° and 178.5° compared to the oxidant soaking structure which had angles of 163.0° and 177.4°. The excess density observed in the proposed intermediate

structure coupled with the well fitting of the electron density and the noticable small changes in heme angles and distance to the cysteine ligated residue are in accordance with a captured intermediate (Figure 6). It should be noted that this intermediate was not seen in the shorter or longer reaction times of the experiments.

Determination of the C-O bond cleavage by ^{18}O labeling studies

To further pinpoint the location of the C-O bond cleavage between an alkyl-O bond (as illustrated in Scheme 1B) or an aromatic carbon-O after hydroxylation reaction, isotope labeling experiments were performed. ^{18}O-labeled water and hydrogen peroxide were employed to identify whether cleavage occurs on the aryl side or the methyl side of the methoxy oxygen, respectively. Concentrated stock solutions of CYP121, peracetic acid, and Tris-HCl buffer pH 7.4 were diluted using ^{18}O-enriched water which made up $\geq$ 85% of the final reaction solution. The product was collected and analyzed via HRMS which yielded an *m/z* of 327 with no ^{18}O incorporation observed, indicating that solvent was unlikely to participate in a nucleophilic attack on the aromatic ring after oxidation similar to what has been observed in the dehaloperoxidase mechanism.[28] Next, ^{18}O-labeled H_2O_2 was employed. A stock solution of $H_2{}^{18}O_2$ was made to 2 mM concentration and added to the reaction mixture in place of peracetic acid as previously described. Again, the product was collected and yielded the same *m*/*z* as has been observed (Figure S1B). This lack of ^{18}O incorporation into the product indicates that after hydrogen atom abstraction, the ferryl-oxo intermediate does not insert itself directly into the aromatic ring, but rather rebounds onto the methylene carbon resulting in deformylation, consistent with the conclusion that C-O bond cleavage occurs on the methyl side of the methoxy oxygen. This is a crucial piece of information for a precise understanding the *O*-demethylation reaction pathway.

The impact of the protonation state and pH

At pH 7.4, the K_D of cYF-4-OMe was determined to be 12.9 ± 0.5 μM by titration (Figure S7), which is comparable to that of cYY. The catalytic shunt pathway was carried out with CYP121 using both cYY and cYF-4-OMe at room temperature in various buffers ranging between pH 7.4 – 10.4 (Figure 7). The reaction with cYY resulted in a single major product, mycocyclosin, which eluted at 4.3 min and has two fewer mass units than cYY and elutes at 6.3 min. Notably, as the pH is increased, nearly full catalytic turnover was observed as shown in Figure 7. This is quite interesting because cYY in pH 10.4 has a K_D value that is ~7 times higher than at pH 7.4, indicating a decreased affinity for the active site when the substrate carries a charge.[15] However, the improved catalytic efficiency of the shunt pathway can potentially be explained by an increased affinity of the peroxide for the iron center, and by the catalytic role of the intact hydroxyl group of cYY. When using as the substrate, the reaction at pH 7.4 using HEPES buffer resulted in a small peak detection at 6.3 min accompanied by many small side product formations, likely from buffer effects. Unlike the reaction with cYY, increasing the pH in the

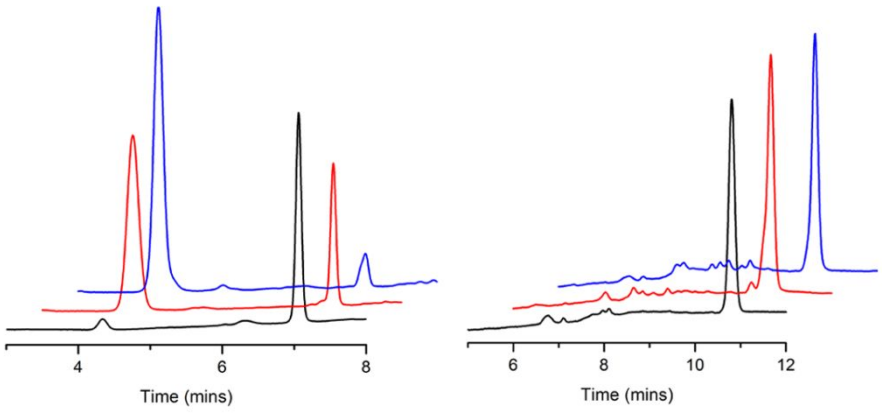

Figure 7. The pH dependence of the CYP121 reaction with cYY or cYF-4-OMe. *Left,* Reaction of CYP121 and cYY using various buffers; 150 mM HEPES buffer pH 7.4 (black), 75 mM CHES buffer pH 9.5 (red), and 150 mM phosphate buffer pH 10.4 (blue). As pH increases, nearly full catalytic turnover is observed, forming the product mycocyclosin at 4.3 min. *Right,* the CYP121 reaction with cYF-4-OMe using the same set of the reported buffers.

cYF-4-OMe reaction did not improve product formation, but rather, resulted in many small side product formations. This observation reinforces the mechanistic proposal that the hydrogen atom present on the hydroxyl group of the substrate dictates the reactivity of the heme-bound oxidant and hence a critical component in the C-C bond coupling reaction.

DISCUSSION

The evidence provided here supports a switch in CYP121 activity from C-C bond coupling of its native substrate to hydroxylation and then *O*-demethylation through oxygen atom insertion into cYF-4-OMe, resulting in a deformylation to release formaldehyde and cYY. By blocking a hydroxyl group of cYY in the probe, the peroxidase-like CYP121 exposes its raw feature as a cytochrome P450 enzyme for its signature hydroxylation reaction and conducts an oxidative C-O bond cleavage reaction through hydroxylation. Though CYP121 performs a peroxidase-like reaction, it is a P450 at heart, possessing the same catalytic power as others to conduct a C-H bond activation, hydroxylation of an alkyl group, and *O*-demethylation. To our knowledge, this *O*-demethylase activity for a P450 enzyme has only been previously observed in a few cases including P450 CYP 1A2 and the newly described CYP 255A (GcoA).[29-30] The structural data obtained in this study show that the sole reason CYP121 performs the chemically easier hydrogen atom abstraction from the phenolic oxygen of cYY rather than electrophilic substitution of the C-H bond site next to the phenol is due to the substrate structure and positioning at the enzyme active site.

Because cYY is an observed product of the cYF-4-OMe reaction mediated by CYP121, the question of why mycocyclosin was not detected as a product naturally arises. During the peroxide shunt reaction with cYF-4-OMe, only a relatively small quantity of cYY would be formed, which is not kinetically competent to outcompete the large excess of cYF-4-OMe. The

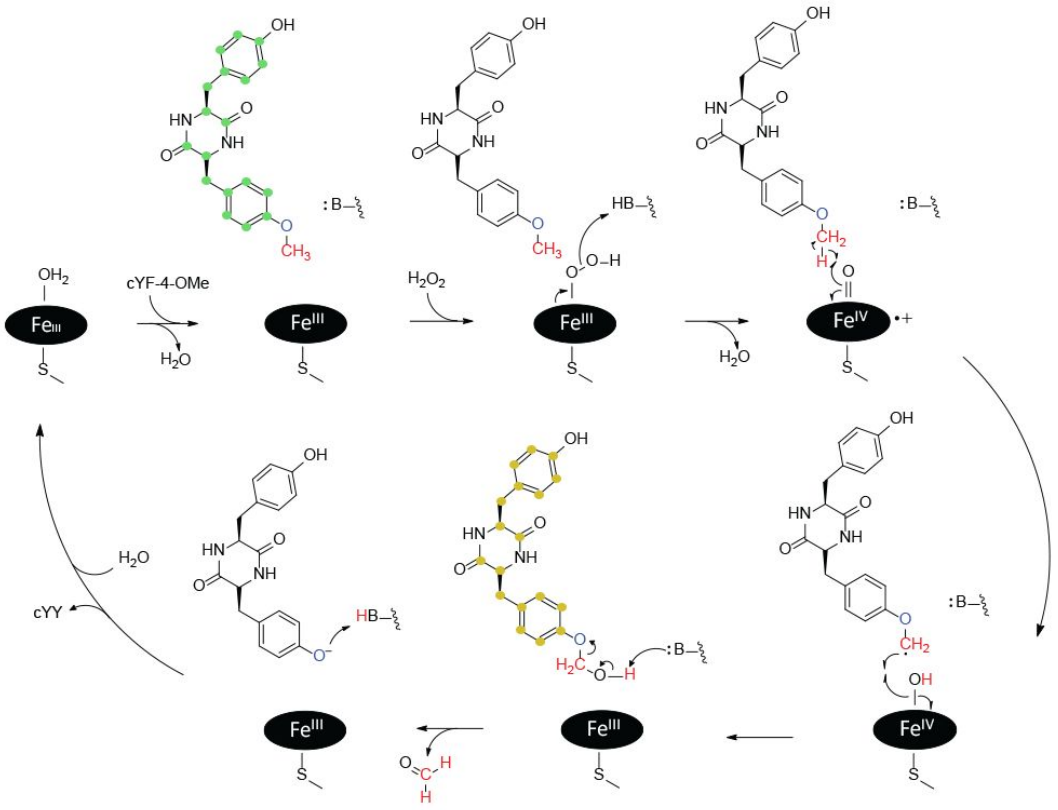

Scheme 2. Proposed mechanistic pathway of CYP121 using cYF-4-OMe as an alternate substrate. The *O*-demethylation of cYF-4-OMe is accomplished through a C-H bond activation and hydroxylation of the methyl group, followed by deformylation. The co-crystallized enzyme-probe complex and the enzyme-intermediate structures are marked with green and yellow carbons respectively. The methoxy oxygen is colored blue and the methyl group is colored red to track the atoms throughout the mechanism.

K_D of cYF-4-OMe (12.9 ± 0.5 μM), compared to our reported K_D of cYY (19.4 ± 0.6 μM[15]) which is in agreement with previously published data,[4] supports this conclusion. The continued exposure to peroxide, as previously shown,[10] damages CYP121, hence reducing the amount of the catalyst and limits the amount of the cYY production in the peroxide shunt reaction.

The results of this study provide the first experimental evidence for (*1*) the importance of the hydrogen atom on the hydroxyl group of cYY for mycocyclosin formation and (*2*) the first putative intermediate crystal structure of CYP121 after the oxidation of an enzyme-substrate complex. As discussed below, these results provide the first line of experimental evidence

supporting that a hydrogen abstraction takes place on the phenolic oxygen of the cYY bound in the enzyme as we have previously proposed,[10] resulting in the formation of a cYY-based radical intermediate for the cyclization reaction to form mycocyclosin.

The observation of apparent demethylation of cYF-4-OMe by HPLC and HRMS could be rationalized by either a peroxidase-like reaction in which a tyrosyl cation radical is attacked by a solvent water molecule or a P450 reaction in which hydrogen atom abstraction followed by oxygen atom rebound on the methyl group precedes deformylation. Thus, the mechanism of demethylation was investigated by product analysis and ^{18}O isotope studies. A peroxidase-like mechanism would require a one- or two-electron oxidation of the 4-*O*-methyltyrosyl moiety by a high-valent iron species followed by nucleophilic attack from solvent water or some iron-oxygen species, resulting in release of methanol. However, when CYP121 reacted with cYF-4-OMe using either ^{18}O-labeled water or peroxide, no isotope enrichment was observed in the product, cYY, eliminating a peroxidase-like mechanism in the CYP121 reaction with cYF-4-OMe. The P450 mechanism for demethylation, however, would not be expected to enrich ^{18}O in the product, but rather a compound I ($Fe(IV)^{+\bullet}=O$) species could initiate a radical reaction with the methyl group by abstraction of a hydrogen atom, forming compound II (Fe(IV)-OH) and leaving a radical on the methylene carbon. The -OH from compound II can then rebound to the methylene radical, forming hydroxylated cYF-4-OMe intermediate, cYF-4-OMeOH, which can then undergo base-catalyzed C-O bond cleavage *via* deformylation. The observation of no isotope scrambling at the methoxy oxygen and quantitative formation of formaldehyde strongly supports the cytochrome P450 mechanism for *O*-demethylation of cYF-4-OMe.

From our proposed mechanism, the initial abstraction of a hydrogen atom from the methyl group by compound I and subsequent oxygen rebound ultimately resulting in

deformylation indicate a hydroxylated probe, cYF-4-OMeOH, as an intermediate. Spontaneous deformylation has not been studied for *O*-methylphenols, though phenoxy 1-methanol has been used in synthetic chemistry[31], therefore cYF-4-OMeOH may be stable enough to be captured, though the question arises of whether or not deformylation is enzymatic. Previously, *O*-dealkylations have been reported to occur from C-H bond hydroxylation of a methyl carbon, resulting in deformylation by other cytochrome P450 enzymes.[32-34] Conversely, horseradish peroxidase utilizes an electron transfer mechanism which causes loss of methanol instead[35], which is not observed for CYP121.

Further evidence for the oxygen-rebound mechanism of the compound II is found in the *in crystallo* reaction studies with H_2O_2. At two min of soaking of the CYP121-(cYF-4-OMe) complex crystals with H_2O_2, excess electron density is observed which connects to the unassigned density on top of the Fe and the methyl carbon of cYF-4-OMe. Fitting the ligand density with cYF-4-OMe resulted in excess electron density on the methyl group, while fitting the ligand density with cYF-4-OMeOH lead to reasonable fitting of the extra density (Figure 5). In its native reaction, CYP121 is expected to deliver two-oxidizing equivalents to cYY. However, steric hindrance of the L-shaped substrate-binding pocket precludes the C-C bond coupling of doubly oxidized cYY (*i.e.*, cY$^{\bullet}$Y$^{\bullet}$). The product mycocyclosin can only be formed during the exit of the postulated cY$^{\bullet}$Y$^{\bullet}$ intermediate. For this reaction, the product-bound structure has not become available either through co-crystallization, soaking, or *in crystallo* chemical reactions, nor any catalytic intermediate after arrival of the oxidant to the ES complex. The cYF-4-OMeOH bound crystal structure of CYP121 represents the first intermediate of the enzyme. Since cYF-4-OMeOH is not anticipated to spontaneously decompose to cYY and formaldehyde under these conditions in the time scale comparable to the solution studies

described above, the subsequent *O*-demethylation is expected be an enzymatic reaction mediated by CYP121 (Scheme 2) as described in CYP 1A2 and 225A.

Due to the unusual, peroxidase-like reaction performed by CYP121 on cYY to form mycocyclosin as well as its ability to robustly perform peroxidase assays, the question arises as to what differentiates CYP121 from more typical cytochromes P450. One potential explanation is that the redox potential of the presumed compound I intermediate that initiates catalysis may be lower than normal so that only a phenolic hydrogen atom could be abstracted, preventing CYP121 from hydroxylating its substrate. This study unexpectedly gauged the magnitude of the power of the enzyme-based oxidant. The observation of oxidative *O*-demethylation activity shows that the redox potential of the CYP121 compound I species suffices for abstraction of a hydrogen atom from carbon. Thus, the factors driving peroxidase-like activity in the native reaction must lie with the active site architecture or dynamics of the enzyme.

CONCLUDING REMARKS

As a potentially druggable enzyme that performs interesting chemistry, CYP121 is ripe for mechanistic investigation. In this study, a substrate analogue was synthesized to probe the reactivity of CYP121. Compared to the native substrate cYY, the asymmetric synthetic probe cYF-4-OMe has a very specific binding mode in CYP121. Unlike cYY, the presence of the methyl group causes a significant low- to high-spin shift upon binding, as observed by EPR, which is not observed for the native substrate. Such a shift is interpreted usually as a departure of the solvent-derived ligand to facilitate the oxidant binding to the iron ion. Various analytical and biochemical methods showed that CYP121 can perform *O*-demethylation *via* a more typical hydroxylation reaction in addition to its normal C-C bond-forming reaction. Mechanistic study

confirmed that the demethylation takes place *via* alkyl hydroxylation of the methoxy group, followed by deformylation. The first intermediate of a P450-catalyzed *O*-demethylation was captured and characterized by X-ray crystallography, which is essential for understanding the *O*-demethylation mechanism mediated by P450 enzymes. This work highlights the importance of the hydroxyl hydrogen of cYY in the formation of mycocyclosin and establishes that CYP121 can mediate C-H bond activation typical of cytochrome P450s in addition to its native peroxidase-like reaction for C-C bond formation.

A common trait of heme enzymes is that they often form a high-valent iron-oxo intermediate which acts as a powerful oxidant. While this species can mediate a remarkable array of oxidation reactions, it is generally true that a given enzyme promotes only a specific type of reaction. How the reaction type is determined after the formation of the key oxidant remains an open question, the answers to which bear on our fundamental understanding of enzyme catalysis as well as *de novo* enzyme design and protein engineering. The study described above indicates that the type of reaction catalyzed by CYP121 is not decided by the heme cofactor alone, and that the substrate plays a role in assisting in directing the oxidizing power to a specific type of chemical reaction. These findings provide insight into the mechanistic determinants of the enzyme for future drug development.

MATERIALS AND METHODS

Chemicals: *N*-Boc-*O*-methyl-L-tyrosine, 98% and L-tyrosine methyl ester hydrochloride, 98% were purchased from Alf Aesar and used as received. All other chemicals were purchased from Sigma Aldrich unless otherwise stated. A CombiFlash Rf+ Flash Chromatography System was used for product purification.

Synthesis of cYF-4-OMe. This compound was synthesized as described with few modifications.[10, 16-17] *N*-Boc-*O*-methyl-L-tyrosine (443 mg, 1.5 mM) was dissolved in 7 mL dimethyl formamide in a 25 mL flask. The flask was charged with L-tyrosine methyl ester hydrochloride (348 mg, 1.5 mM), stirred until fully dissolved, and warmed to 60°C. Diisopropylethylamine (523 µL, 3.0 mmol) and HATU (627 mg, 1.7 mM), purchased from Combi-blocks, was added. The air in the flask was exchanged with argon and left to stir for 4 hrs. The reaction was quenched with ethyl acetate and washed with sodium bicarbonate, brine, and dried with sodium sulfate. The organic solvent was removed *in vacuo* and resulting cream colored solid was purified with a flash column using a gradient of ethyl acetate in hexane from 5% to 85% over a period of 20 min. The product was collected in 5 mL test tubes, combined, and solvent was removed *in vacuo*. The resulting white solid was then dissolved in formic acid (5 mL/mM) and monitored via TLC until fully deprotected. The formic acid was removed *in vacuo*. The flask was charged with a mixture of *sec*-butanol and toluene (5:1) and heated to 105°C for 2h. The resulting crystallized white solid was filtered out and washed with ethyl acetate (85%, 434 mg, 1.3 mmol), $[MH]^+$ *m/z* 341.1339, ^{1}H NMR (300 MHz, DMSO-d_6) δ ppm 2.06 - 2.26 (m, 2 H) 2.53 - 2.61 (m, 2 H) 3.70 (s, 3 H) 3.88 (br. s., 2 H) 6.68 (m, *J*=8.20 Hz, 2 H) 6.85 (d, *J*=8.20 Hz, 4 H) 6.91 - 7.00 (m, 2 H) 7.81 (d, *J*=6.44 Hz, 2 H) 9.21 (s, 1 H).

Enzyme overexpression and purification. Expression and purification of CYP121 from *Mycobacterium tuberculosis* has been described elsewhere. CYP121 was purified as described with minor modification.[10] A starter culture was made using a 250 mL flask containing 150 mL LB media culture mixed with kanamycin (100 µM). A starter culture *E. coli* bearing the CYP121 expression plasmid was made from glycerol stock stored at -80°C. An autoclaved flask with LB broth was inoculated and cultured for 24 h in an incubator at 220 rpm and 37 °C. The next day,

the starter culture was used to inoculate 11, 1 L LB/kanamycin cultures which were then grown at 220 rpm and 37 °C until an OD_{600} of ~0.9 was reached. At this point, δ-aminolevulinic acid (300 μM), iron (II) ammonium sulfate (35 μM), and isopropyl β-D-1-thiogalactopyranoside (400 μM) was added and the incubation temperature decreased to 28°C. The cultures were grown for 16 h before being harvested via centrifugation (3700 rcf) for 12 min.

The pellet was resuspended in lysis buffer (50 mM Tris, pH 8.0, 200 mM NaCl, 5% glycerol) and passed through a Microfluidics LS-20 cell disrupter (30,000 psi). The cell debris was then pelleted by centrifugation (2 × 34,000 g for 40 min) and the lysate was loaded onto a Ni-NTA affinity column. Before loading, the column was prepared using 500 mM imidazole buffer (50 mM Tris-HCl, pH 8.0, 200 mM NaCl, 5% glycerol) to remove non-specifically bound protein. The column was re-equilibrated with buffer not containing imidazole and the lysate was loaded onto the column (1.2 mL/min) and washed with buffer (1.5 mL/min). After the protein is fully loaded, 15 mM imidazole buffer was used to wash the column until a peak consisting of weakly bound protein is eluted. A gradient from 20 mM to 425 mM imidazole is used over 120 mL to elute CYP121. Five fractions were collected, the first two and last three pooled and concentrated separately using a 30 kDa membrane. The protein was then desalted using a Sephadex G-25 desalting column using 50 mM Tris-HCl, pH 7.4. The fractions containing protein were collected and concentrated and protein and heme concentration was determined using ε_{280} = 26 500 M^{-1} cm^{-1} and ε_{416} = 110 000 M^{-1} cm^{-1}. The purified protein was concentrated to ~700 μM and heme occupancy averaged 55% [heme]/[protein] as determined by UV-vis. Purified protein was frozen in liquid nitrogen and stored at -80 °C until needed.

Reaction setup and HPLC analysis. Reactions and HPLC analysis were conducted at room temperature in 50 mM Tris-HCl, pH 7.4. cYF-4-OMe was dissolved in DMSO to make a 27 mM

stock solution. The stock of peracetic acid (2 mM) was made and titrated into the reaction mixture. CYP121 (50 or 500 μM) was incubated with cYF-4-OMe (600 μM) for 5 min before peracetic acid (300 μM) was titrated over a 15-minute period to avoid rapid heme bleaching. Four controls were considered: i) CYP121 only, ii) CYP121 and cYF-4-OMe, iii) CYP121 and peracetic acid, and iv) cYF-4-OMe and peracetic acid.

The enzyme was then filtered out using a 10 kDa concentrator (Millipore) at 15,000×*g* over a period of 20 min. 50 μL was injected onto an Inert Sustain C18 column (5 μM particle size, 4.6 X 100 mm, GL Sciences Inc.) and analyzed *via* a Thermo Scientific Ultimate-3000SD HPLC rapid separation system equipped with a photodiode array detector. The product was collected from the HPLC for analysis by UV-vis spectroscopy (Agilent 8453 UV-Visible spectrophotometer).

EPR of Fe(III)-CYP121: CYP121, CYP121-cYF-4-OMe, CYP121-cYY complexes. EPR samples of CYP121 were prepared from a 200 μM enzyme solution in 50 mM Tris-HCl, pH 7.4 and flash-frozen in liquid ethane over a liquid nitrogen bath and stored in liquid nitrogen until measurement. CYP121-substrate complexes were prepared by incubating 200 μM CYP121 with either 700 μM cYY or 400 μM cYF-4-OMe and flash frozen and stored as previously described. EPR spectra for **E** and **ES** complexes were collected with a Bruker E560 spectrometer. Temperature was controlled with a cryogen-free system. Measurements were made in a SHQE-W resonator at 9.4 GHz, with 100 kHz modulation frequency and 0.6 mT modulation amplitude. Data were collected at 10K, 1.002 mW and 50 K, 0.200 mW microwave power.

Secondary product identification. Alcohol dehydrogenase from *Saccharomyces Cerevisiae* (yeast) was purchased from Sigma Aldrich as a lyophilized powder and used as received. ~50 units of ADH were mixed with 200 μM NADH and 400 μL CYP121 reaction flow through from

the previous section. The absorbance was monitored at 339 nm using a UV-vis spectrophotometer (Agilent 8453) during the reaction.

Formaldehyde dehydrogenase from *Pseudomonas* was purchased from Sigma Aldrich as a lyophilized powder and used as received. ~0.5 units of FDH were mixed with 200 μM NAD^+ and CYP121 reaction flow through and the reaction was monitored as described above.

Chemical method of formaldehyde formation quantitation was also attempted. 2, 4-dinitrophenylhydrazine (2, 4-DNP) was purchased from Sigma Aldrich and prepared using previously published methods.[27] The reaction of CYP121 with cYF-4-OMe was completed as described above, heated to precipitate the enzyme, and then the solids were pelleted. The supernatant was collected and 2, 4-DNP was added to make up 1.5 % of the mixture. The resulting mixture was then analyzed via HPLC utilizing a gradient of 5 – 95% acetonitrile in H_2O with 0.1% formic acid.

^{18}O incorporation analyses. ^{18}O-water and ^{18}O-hydrogen peroxide were purchased from Sigma Aldrich. For ^{18}O H_2O_2 experiments, the reaction set up is as described above. $H_2{}^{18}O_2$ (300 μM) was titrated into a solution of CYP121 (50 μM) and cYF-4-OMe (700 μM) in 50 mM Tris-HCl, pH 7.4 over a period of 15 minutes. The enzyme was then removed via a 10 kDa concentrator (Millipore), analytes separated on HPLC, product collected and analyzed via HRMS.

For the ^{18}O water experiments, a 1 M buffer solution (50 mM Tris-HCl, pH 7.4), and stock solution of peracetic acid was made by diluting with isotopically labeled water where the ^{18}O water did not make up less than 85% of the total solution. From this, the reaction was conducted and analyzed as previously described.

pH Dependence study. The following buffers were used for pH-dependent experiments; 150 mM HEPES buffer pH 7.4; 75 mM *N*-cyclohexyl-2-aminoethanesulfonic acid (CHES), pH 9.5; and 150 mM phosphate buffer, pH 10.4.

Crystallization, *in crystallo* chemical reaction, X-ray data collection, and data analyses. Crystals of the CYP121-cYF-4-OMe complex were obtained using the hanging drop method. The N-terminal His_6-tagged enzyme was cleaved using a Thrombin CleanCleave Kit (Sigma Aldrich) prior to crystallization. The enzyme buffer consisted of 50 mM Tris-HCl pH 7.4. Crystallization condition conditions consisted of 100 mM MES pH 5.0 – 5.7 and 1.85 – 2.05 M ammonium sulfate with 600 μM cYY or 400 μM cYF-4-OMe at 6 °C in a vibration -free crystallization refrigerator. The protein was mixed in a 1:1 ratio with the crystallization solution for a total volume of 2 μL and the crystals began appearing after 1.5 weeks.

To increase the pH of the crystals to 7.4, four incremental solutions of 100 mM MES, pH 5.9 – 7.4 were made with 2.0 M ammonium sulfate. Crystals were soaked in increasing pH crystallization solutions for 20 minutes until pH 7.4. To obtain an intermediate complex, crystals were picked and placed into 25 μL of cryoprotectant containing 100 mM MES, pH 7.4, 2.0 M ammonium sulfate, and 20% glycerol. H_2O_2 was added to the cryoprotectant at a final concentration of 5 mM and gently mixed. Crystals were mounted onto loops and stored in liquid nitrogen at various times ranging from 30 s – 10 min.

X-ray diffraction data were collected at the beamline 9-2 of The Stanford Synchrotron Radiation Lightsource (SSRL), National Accelerator Laboratory (SLAC) for the co-crystallization complex and at Argonne National Laboratory Advanced Photon Source (APS) beamline 19-BM. Diffraction data were collected at 1.0 Å wavelength with a Dectris Pilatus 6M detector (SSRL) or ADSC Quantum 315r detector (APS) and the crystal was kept under a

nitrogen stream at 100 K. The data were processed with HKL3000. The structure was solved using Phaser-MR[36] molecular replacement software and 5WP2.pdb[15] as the search template and refined in the Phenix[37] program package. Ligands including heme and cYF-4-OMe for the co-crystallization structure were observed at 100% occupancy within the active site after data collection, molecular replacement, and refinement. H_2O_2 soaking experiments were observed at 98% occupancy after refinement. Water molecules were adding during the final refinement and WinCoot[38] and PyMOL[39] were used for structure modeling.

■ ASSOCIATED CONTENT

AUTHOR INFORMATION

Corresponding Author

* A.L.: tel, +1-210-458-7062; fax, 210-458-7428; e-mail, Feradical@utsa.edu; web, http://Feradical.utsa.edu

ORCID

Romie C. Nguyen: 0000-0002-9450-2364

Yu Yang: 0000-0001-5305-2435

Yifan Wang: 0000-0003-0378-2469

Ian Davis: 0000-0002-1566-4972

Aimin Liu: 0000-0002-4182-8176

Notes

The authors declare no competing financial interest.

Supporting Information

The Supporting Information is available free of charge on the ACS Publications website at DOI: xxxx

Synthetic scheme for cYF-4-OMe (Scheme S1), ^{1}H-NMR and high-resolution mass spectrometry (Figure S1) of the synthetic probe, the calibration curves of cYY and NADH (Figure S2), alcohol dehydrogenase control with NADH (Figure S3), heme ruffle of CYP121 in the captured intermediate cYF-4-OMeOH structure relative to the co-crystallized enzyme in complex with cYF-4-OMe (Figure S4), determination of the binding affinity of CYP121 with cYF-4-OMe (Figure S5).

Acknowledgement

This work was financially supported by the National Institutes of Health (NIH) grant R01GM108988 and the Lutcher Brown Endowment fund (to A.L.). We are indebted to Prof. Stanton F. McHardy for constructive discussions of the synthetic strategy of the mechanistic probe. Mr. Li Ma is acknowledged for the participation of the early stage of this study. We thank the staff scientists at the sections 19 beamline of the Advanced Photon Source (APS), Argonne National Laboratory and the beamline 9–2 of the Stanford Synchrotron Radiation Lightsource (SSRL), SLAC National Accelerator Laboratory. Use of the APS and SSRL is supported by the U.S. Department of Energy, Office of Science, Office of Basic Energy Sciences, under Contracts DE-AC02-06CH11357 and DE-AC02-76SF00515, respectively. The SSRL facility is additionally supported by National Institutes of Health Grant P41GM103393.

REFERENCE

1. McLean, K. J.; Carroll, P.; Lewis, D. G.; Dunford, A. J.; Seward, H. E.; Neeli, R.; Cheesman, M. R.; Marsollier, L.; Douglas, P.; Smith, W. E.; Rosenkrands, I.; Cole, S. T.; Leys, D.; Parish, T.; Munro, A. W. Characterization of Active Site Structure in CYP121. A Cytochrome P450 Essential for Viability of *Mycobacterium tuberculosis* H37Rv. *J. Biol. Chem.* **2008,** *283*, 33406-33416.
2. Ortiz de Montellano, P. R. Potential Drug Targets in the *Mycobacterium tuberculosis* Cytochrome P450 System. *J. Inorg. Biochem.* **2018,** *180*, 235-245.
3. Guengerich, F. P.; Munro, A. W. Unusual Cytochrome P450 Enzymes and Reactions. *J. Biol. Chem.* **2013,** *288*, 17065-17073.
4. Belin, P.; Le Du, M. H.; Fielding, A.; Lequin, O.; Jacquet, M.; Charbonnier, J. B.; Lecoq, A.; Thai, R.; Courçon, M.; Masson, C.; Dugave, C.; Genet, R.; Pernodet, J. L.; Gondry, M. Identification and Structural Basis of the Reaction Catalyzed by CYP121, an Essential Cytochrome P450 in *Mycobacterium tuberculosis*. *Proc. Natl. Acad. Sci. U.S.A.* **2009,** *106*, 7426-7431.
5. Guengerich, F. P.; Yoshimoto, F. K. Formation and Cleavage of C-C Bonds by Enzymatic Oxidation-Reduction Reactions. *Chem. Rev.* **2018,** *118*, 6573-6655.
6. Makino, M.; Sugimoto, H.; Shiro, Y.; Asamizu, S.; Onaka, H.; Nagano, S. Crystal Structures and Catalytic Mechanism of Cytochrome P450 StaP that Produces the Indolocarbazole Skeleton. *Proc. Natl. Acad. Sci. U.S.A.* **2007,** *104*, 11591-11596.
7. Amann, T.; Zenk, M. H. Purification and Characterization of a Cytochrome P450 Enzyme From Pig Liver: Catalyzing the Phenol Oxidative Coupling of (*R*)-Reticuline to Salutaridine, the Critical Step in Morphine Biosynthesis. *Tetrahedron Lett.* **1991,** *32*, 3675-3678.
8. Grobe, N.; Zhang, B.; Fisinger, U.; Kutchan, T. M.; Zenk, M. H.; Guengerich, F. P. Mammalian Cytochrome P450 Enzymes Catalyze the Phenol-Coupling Step in Endogenous Morphine Biosynthesis. *J. Biol. Chem.* **2009,** *284*, 24425-24431.

9. Pylypenko, O.; Vitali, F.; Zerbe, K.; Robinson, J. A.; Schlichting, I. Crystal Structure of OxyC, a Cytochrome P450 Implicated in an Oxidative C-C Coupling Reaction During Vancomycin Biosynthesis. *J. Biol. Chem.* **2003,** *278*, 46727-46733.

10. Dornevil, K.; Davis, I.; Fielding, A. J.; Terrell, J. R.; **Liu, A.** Crosslinking of Dicyclotyrosine by the Cytochrome P450 Enzyme CYP121 from *Mycobacterium tuberculosis* Proceeds Through a Catalytic Shunt Pathway. *J. Biol. Chem.* **2017,** *292*, 13645-13657.

11. Dumas, V. G.; Defelipe, L. A.; Petruk, A. A.; Turjanski, A. G.; Marti, M. A. QM/MM Study of the C−C Coupling Reaction Mechanism of CYP121, an Essential Cytochrome P450 of *Mycobacterium tuberculosis*. *Proteins* **2014,** *82*, 1004-1021.

12. Yukl, E. T.; Liu, F.; Krzystek, J.; Shin, S.; Jensen, L. M. R.; Davidson, V. L.; Wilmot, C. M.; **Liu, A.** Diradical Intermediate Within the Context of Tryptophan Tryptophylquinone Biosynthesis. *Proc. Natl. Acad. Sci. U.S.A.* **2013,** *110*, 4569-4573.

13. Conner, K. P.; Schimpf, A. M.; Cruce, A. A.; McLean, K. J.; Munro, A. W.; Frank, D. J.; Krzyaniak, M. D.; Ortiz de Montellano, P.; Bowman, M. K.; Atkins, W. M. Strength of Axial Water Ligation in Substrate-Free Cytochrome P450s is Isoform Dependent. *Biochemistry* **2014,** *53*, 1428-1434.

14. Luthra, A.; Denisov, I. G.; Sligar, S. G. Spectroscopic Features of Cytochrome P450 Reaction Intermediates. *Arch. Biochem. Biophys.* **2011,** *507*, 26-35.

15. Fielding, A. J.; Dornevil, K.; Ma, L.; Davis, I.; **Liu, A.** Probing Ligand Exchange in the P450 Enzyme CYP121 from *Mycobacterium tuberculosis*: Dynamic Equilibrium of the Distal Heme Ligand as a Function of pH and Temperature. *J. Am. Chem. Soc.* **2017,** *139*, 17484-17499.

16. He, C.; Stratton, T. P.; Baran, P. S. Concise Total Synthesis of Herqulines B and C. *J. Am. Chem. Soc.* **2019,** *141*, 29-32.

17. Jung, M. E.; Rohloff, J. C. Organic Chemistry of L-Tyrosine. 1. General Synthesis of Chiral Piperazines from Amino Acids. *J. Organ. Chem.* **1985,** *50*, 4909-4913.

18. Denisov, I. G.; Makris, T. M.; Sligar, S. G.; Schlichting, I. Structure and Chemistry of Cytochrome P450. *Chem. Rev.* **2005,** *105*, 2253-2277.

19. Orme-Johnson, N. R.; Orme-Johnson, W. H. In *Methods in Enzymology*, Fleischer, S., Packer, L., Eds. Academic Press, New York: **1978**; Vol. 52, pp 252-257.

20. Fonvielle, M.; Du, L. M. H.; Lequin, O.; Lecoq, A.; Jacquet, M.; Thai, R.; Dubois, S.; Grach, G.; Gondry, M.; Belin, P. Substrate and Reaction Specificity of *Mycobacterium tuberculosis* Cytochrome P450 CYP121 Insights from Biochemical Studies and Crystal Structures. *J. Biol. Chem.* **2013,** *288*, 17347-17359.

21. Karplus, P. A.; Diederichs, K. Linking Crystallographic Model and Data Quality. *Science* **2012,** *336*, 1030-1033.

22. Engh, R. A.; Huber, R. Accurate bond and angle parameters for X-ray protein structure refinement. *Acta Cryst. A* **1991,** *47*, 392-400.

23. Chen, V. B.; Arendall, W. B., III; Headd, J. J.; Keedy, D. A.; Immormino, R. M.; Kapral, G. J.; Murray, L. W.; Richardson, J. S.; Richardson, D. C. MolProbity: all-atom structure validation for macromolecular crystallography. *Acta Cryst. D* **2010,** *66*, 12-21.

24. Abeles, R. H.; Lee, H. A. The Dismutation of Formaldehyde by Liver Alcohol Dehydrogenase. *J. Biol. Chem.* **1960,** *235*, 1499-1503.

25. Mani, J.-C.; Pietruszko, R.; Theorell, H. Methanol Activity of Alcohol Dehydrogenases from Human Liver, Horse Liver, and Yeast. *Arch. Biochem. Biophys.* **1970,** *140*, 52-59.

26. Zilly, F. E.; Acevedo, J. P.; Augustyniak, W.; Deege, A.; Hausig, U. W.; Reetz, M. T. Tuning a P450 Enzyme for Methane Oxidation. *Angew. Chem. Int. Ed. Engl.* **2011,** *50* , 2720-2724.

27. Ruekberg, B.; Rossoni, E. An Improved Preparation of 2, 4-Dinitrophenylhydrazine Reagent. *J. Chem. Ed.* **2005,** *82*, 1310.

28. Osborne, R. L.; Coggins, M. K.; Raner, G. M.; Walla, M.; Dawson, J. H. The Mechanism of Oxidative Halophenol Dehalogenation by Amphitrite ornata Dehaloperoxidase Is Initiated by H_2O_2

Binding and Involves Two Consecutive One-Electron Steps: Role of Ferryl Intermediates. *Biochemistry* **2009,** *48*, 4231-4238.

29. Mallinson, S. J. B.; Machovina, M. M.; Silveira, R. L.; Garcia-Borras, M.; Gallup, N.; Johnson, C. W.; Allen, M. D.; Skaf, M. S.; Crowley, M. F.; Neidle, E. L.; Houk, K. N.; Beckham, G. T.; DuBois, J. L.; McGeehan, J. E. A Promiscuous Cytochrome P450 Aromatic *O*-Demethylase for Lignin Bioconversion. *Nat. Commun.* **2018,** *9*, 2487.
30. Yun, C.-H.; Miller, G. P.; Guengerich, F. P. Oxidations of *p*-Alkoxyacylanilides Catalyzed by Human Cytochrome P450 1A2: Structure−Activity Relationships and Simulation of Rate Constants of Individual Steps in Catalysis. *Biochemistry* **2001,** *40*, 4521-4530.
31. Rajak, H.; Veerasamy, R.; Gupta, A. K.; Kharya, M. D.; Mishra, P. Synthesis and Pharmacological Evaluation of New Indolyl-Oxadiazoles as Anticonvulsant Agents. *Int. J. Pharm. Sci. Nantechnol.* **2009,** *2*, 661-666.
32. Guengerich, F. P. Common and Uncommon Cytochrome P450 Reactions Related to Metabolism and Chemical Toxicity. *Chem. Res. Toxicol.* **2001,** *14*, 611-650.
33. Ortiz de Montellano, P. R.; De Voss, J. J. Oxidizing Species in the Mechanism of Cytochrome P450. *Nat. Prod. Rep.* **2002,** *19*, 477-493.
34. Yun, C.-H.; Miller, G. P.; Guengerich, F. P. Rate-Determining Steps in Phenacetin Oxidations by Human Cytochrome P450 1A2 and Selected Mutants. *Biochemistry* **2000,** *39*, 11319-11329.
35. Meunier, G.; Meunier, B. Peroxidase-Catalyzed *O*-Demethylation Reactions. Quinone-Imine Formation from 9-Methoxyellipticine Derivatives. *J. Biol. Chem.* **1985,** *260*, 10576-10582.
36. McCoy, A. Solving Structures of Protein Complexes by Molecular Replacement with Phaser. *Acta Cryst. D* **2007,** *63*, 32-41.
37. Adams, P. D.; Afonine, P. V.; Bunkoczi, G.; Chen, V. B.; Davis, I. W.; Echols, N.; Headd, J. J.; Hung, L.-W.; Kapral, G. J.; Grosse-Kunstleve, R. W.; McCoy, A. J.; Moriarty, N. W.; Oeffner, R.; Read, R. J.; Richardson, D. C.; Richardson, J. S.; Terwilliger, T. C.; Zwart, P. H. PHENIX: A

Comprehensive Python-Based System for Macromolecular Structure Solution. *Acta Cryst. D* **2010,** *66*, 213-221.

38. Emsley, P.; Lohkamp, B.; Scott, W. G.; Cowtan, K. Features and Development of Coot. *Acta Crysta. D* **2010,** *66*, 486-501.

39. Delano, W. L. The PyMOL Molecular Graphics System, Version 2.3.3.0. *Schrodinger, LLC, New York* **2014**.

For Table of Contents Only